

Appendix B

Bulk Mn₃Si

The cubic crystal structure of Mn₃Si and its iso-structures, e.g. Fe₃Si and Fe₂MnSi, is called DO_3 type structure. Their crystals are equivalent to the $L2_1$ structure of the Heusler compounds¹ X_2YZ [165] Fig. B-4-a. Metallic Mn₃Si crystallizes as Mn_I-Mn_{II}-Si with space group $Fm\bar{3}m$ and has complex spin configuration which depends on the temperature. Despite of its complex magnetic structure, Mn₃Si is an itinerant electron antiferromagnet with incommensurate magnetic structure [154, 166] at 25 K. At this temperature, it has in-plane magnetic moments of $\mu_I = 1.7 \mu_B$ and $\mu_{II} = -0.19 \mu_B$ [154]. The crystal structure can be described in terms of an fcc Bravais lattice with Si atoms at the fcc lattice sites and Mn atoms occupying all of the octahedral and tetrahedral sites of the lattice. The Si and Mn_I atoms are located at $(0, 0, 0)$ and $(\frac{1}{2}, \frac{1}{2}, \frac{1}{2})$, respectively, while the Mn_{II} atoms occupy $(\frac{1}{4}, \frac{1}{4}, \frac{1}{4})$ and $(\frac{3}{4}, \frac{3}{4}, \frac{3}{4})$ sites. The Mn_I sites are surrounded by eight Mn_{II} nearest neighbors and the nearest neighbors of Mn_{II} are four Mn_I and four Si atoms.

The calculations for non-magnetic, ferromagnetic and antiferromagnetic types of ordering are performed and the results are compared with those from the literature. The ferromagnetic ordering is described as a sequence of ferromagnetic planes Mn_{II}-Mn_I-Mn_{II}, separated by a Si plane, all equidistant with $d = 1.4 \text{ \AA}$. In the antiferromagnetic phase, it is assumed that the magnetic moments of the Mn_I and the Mn_{II} have an antiparallel coupling.

The calculations concerning the structural, electronic and magnetic properties are done with the GGA functional, an energy cutoff of $E_{\text{cut}} = 13.6 \text{ Ry}$ and $17 \times 17 \times 17$ \mathbf{k} -points in the Brillouin zone.

B-1 Structural and Magnetic Properties

The energy vs. volume plots are shown in Fig. B-4-b as green, red, blue curves for nonmagnetic (NM), ferromagnetic (FM) and antiferromagnetic (AFM) ordering, respectively. As these curves show, the AFM spin configuration has the lowest energy. At a compressed volume of -14 % the system becomes non-magnetic.

¹The Heusler alloys have half metallic behavior: The Fermi level lying in the band gap in the minority spin channel and the electronic bandstructure of majority spin, like metallic bandstructure, crosses Fermi level which cause higher mobility and conductivity in this channel.

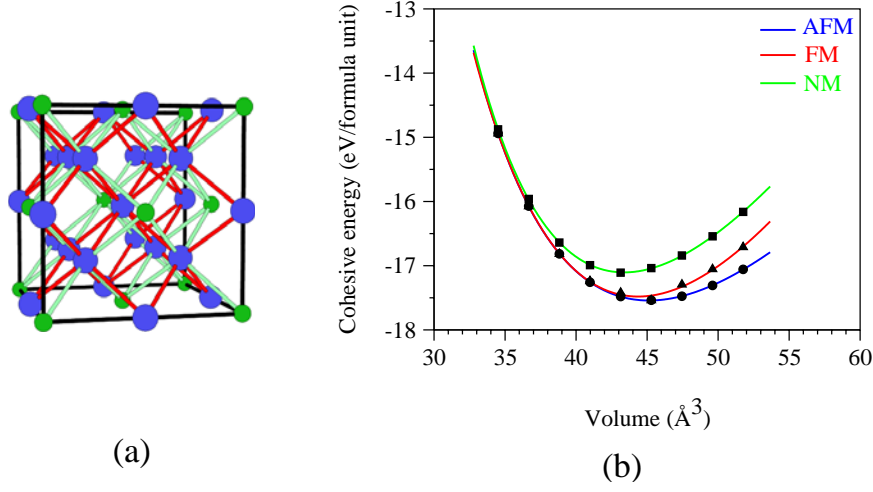


Fig. B-4: Crystal structure of Mn₃Si in the fcc lattice (a). The green small circles are Si and big blue circles are Mn. Energy-volume curves for non-magnetic, ferromagnetic and antiferromagnetic structures for Mn₃Si (b). The antiferromagnetic structure has the lowest energy curve.

Therefore one can conclude a magnetic phase transition to the non-magnetic phase at the compressed volume.

The stability of the AFM phase can be explained by direct $d-d$ coupling between Mn_I and Mn_{II}, which lowers the energy in the antiparallel spin alignment. The calculated and experimentally observed lattice constants and magnetic moments for this crystal are summarized in Table B-1.

Table B-1: Formation enthalpy (ΔH) (cf. Eq. ??), lattice parameter (a_0) and magnetic moments (m_I , m_{II}) of Mn_I and Mn_{II} in different layers for Mn₃Si.

Mn ₃ Si fcc	Phase	ΔH [eV/formula unit]	a_0 [Å]	m_I [μ_B]	m_{II} [μ_B]
Present work (GGA)	AFM	1.15	5.65	2.15	-0.30
	FM	1.093	5.62	2.58	0.83
	NM	0.72	5.59	—	—
LMTO(LSDA) ^(a)	AFM	—	5.63	2.06	-0.43
EXP. ^(b)	AFM	—	5.72	1.7	-0.19

(a) Ref. [167]

(b) Ref. [154]

The results for the magnetic moments are similar to LMTO results [167], and are overestimated compared to experimental magnetic moments, but both method pre-

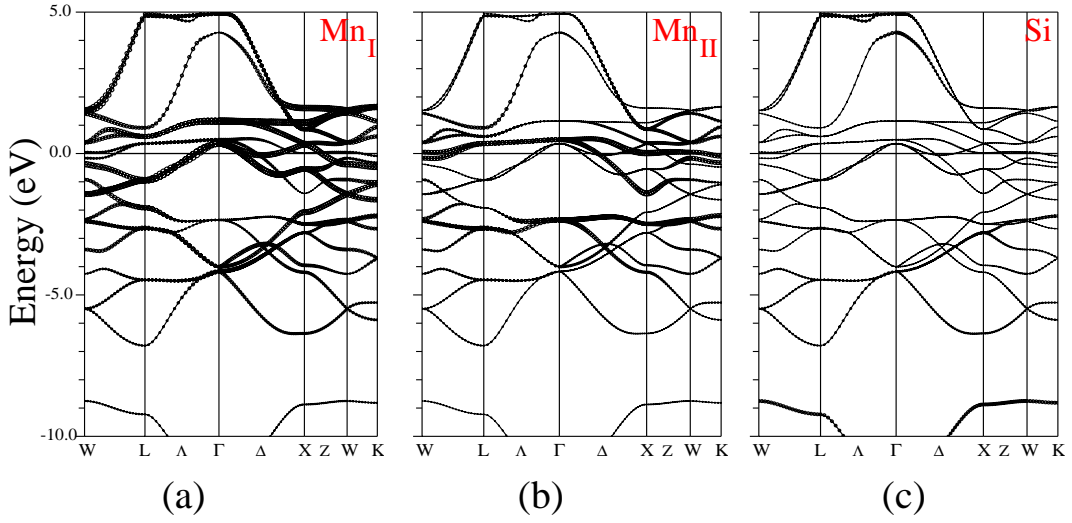


Fig. B-5: Band structure of non-magnetic Mn_3Si shows metallic behavior. The contributions of Mn_I (a), Mn_{II} (b) and Si (c) atoms are shown separately.

dict antiferromagnetic ordering.

B-2 Electronic Properties

The electronic properties are studied by analyzing the band structures of non-magnetic, Fig. B-5, and antiferromagnetic Mn_3Si , Fig. B-6. Figures (a), (b), and (c) in Fig. B-5 show the bands weighted with their projection onto the atomic orbitals of Mn_I , Mn_{II} and Si, respectively in the non-magnetic structure. Their corresponding AFM band structures, Fig. B-6, show the majority (a-c) and minority (d-f) spin channels. [The thickness of the bands of each atom indicates the contribution of the specific atom to the particular band.]

In all graphs the Mn_I atoms considerably contribute around the Fermi level, whereas the Si p-states are far from the Fermi level. This means the magnetic ordering has no effect on the character of the p-bands.

A comparison of the band structures of NM and AFM at their equilibrium volume show that, the bands below -3 eV and above 1 eV are identical for both magnetic structures. As an example, the bands around the Fermi level at the Γ point are considered, c.f. Fig. B-6. Both the NM phase and the majority spin channel of the AFM phase exhibit metallic behavior. There is an exchange splitting of the Mn 3d-electron states in the magnetic structure and the Γ_{12} level is shifted below the Γ_{25} band due to polarization. The Mn_{II} , which has O_h symmetry, tends to be polarized strongly far away from the Fermi level which results in an indirect gap of about 0.5 eV in the minority spin channel. The Fermi level touches the top of the valence band at the point Γ . For this reason, this material does not belong to the group of half-metal compounds.

The bands in the energy range of -3 to 1 eV have mainly *d*-character. The Γ_{12} and

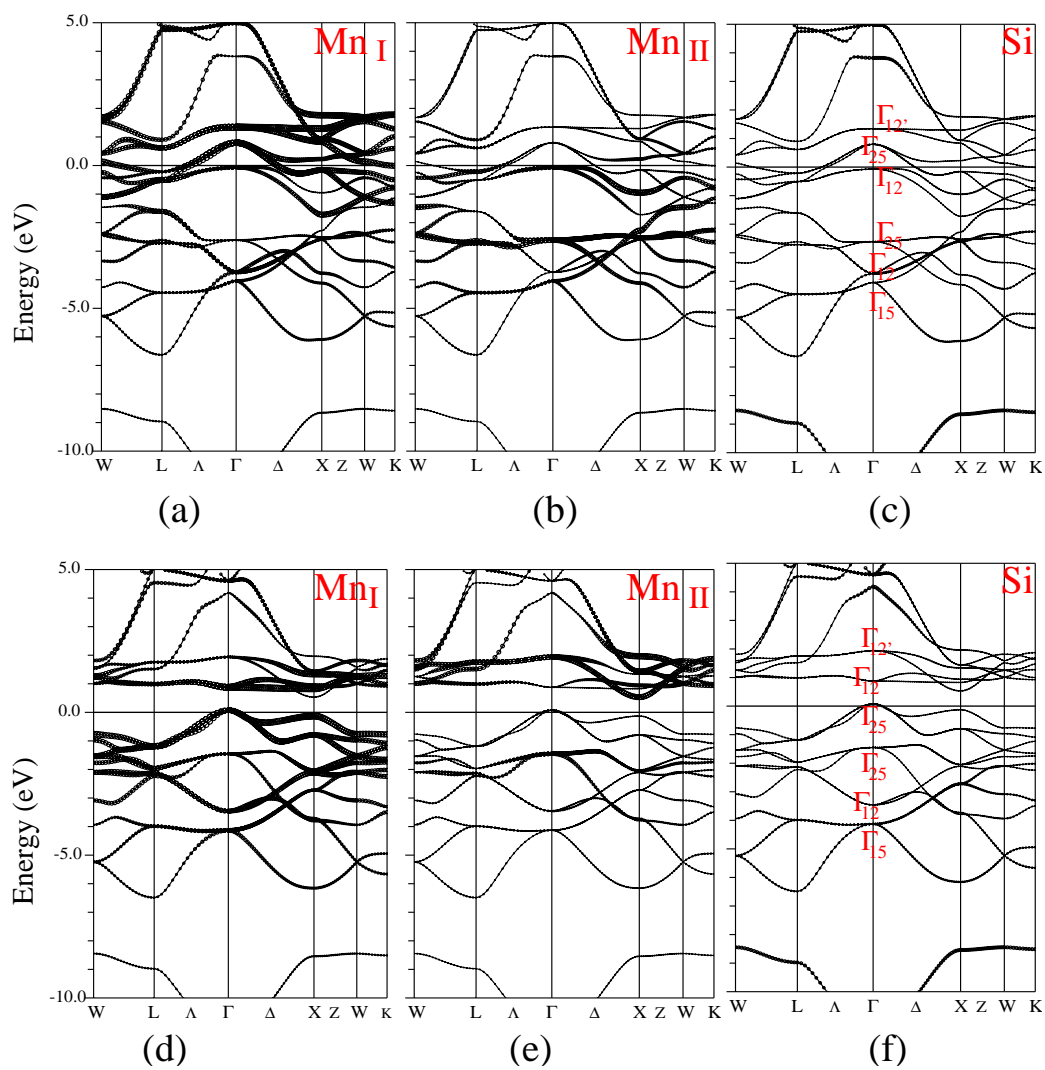


Fig. B-6: Band structures for Mn_I, Mn_{II} and Si atoms in majority spin direction (a, b, c) and for minority spin channel (d, e, f) of Mn₃Si in the AFM phase. The majority spin band structure has the Fermi level crosses the top of the conduction band at the high symmetry point Γ which produce a few hole in this band.

Γ_{15} bands have e_g and t_{2g} symmetry of the d -orbitals, respectively [168].

The lower e_g and t_{2g} level belong to Mn_I sites and the Γ_{12} and Γ_{25} levels, which have the same symmetry of d - Mn_{II} are near to the Fermi level, see Figs. B-5 and B-6. Therefore the energy level of d - Mn_I is lower than d - Mn_{II} . The d -orbitals of Mn atoms, which possess similar symmetry will overlap, thereby broadening these bands. The obvious differences between the polarized and non-polarized band structure can be seen in the Γ_{12} , Γ_{25} and $\Gamma_{12'}$ levels. There is a strong separation between in the minority spin channel of Γ_{12} , Γ_{25} into antibonding and bonding states, respectively. The Γ_{12} which is located above Γ_{25} band is shifted to lower energy and ends up below the Fermi level in the majority spin channel. It is also remarkable that contributions of d - Mn_{II} in on $\Gamma_{12'}$ band becomes negligible. Therefore the latter band is rather flat in spinpolarized calculations.

Figure B-7 illustrates the density of states for total and constituent parts of the crystal in the FM and AFM magnetic phases using the tetrahedral integration method [169, 170].

The Γ_{12} and Γ_{25} levels below and above the Fermi level in the spinpolarized band structure lead to two clear peaks in the DOS plot of Mn_{II} atoms, Fig. B-7.

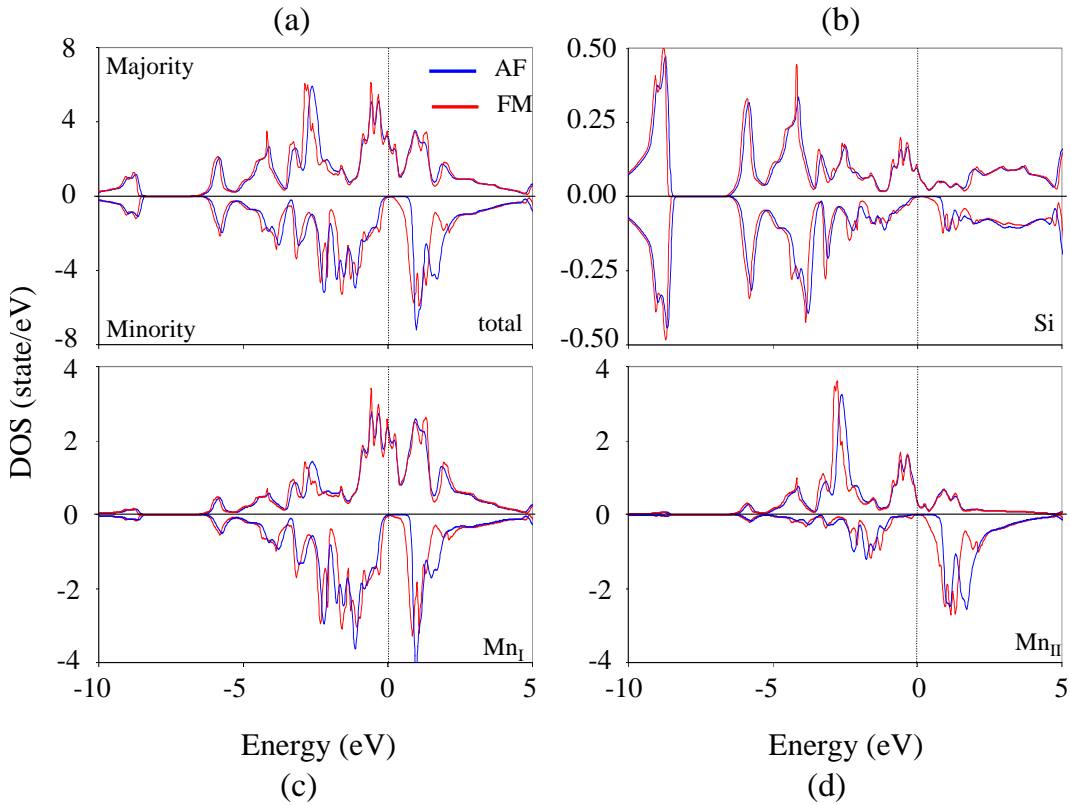


Fig. B-7: The DOS plot of Mn_3Si for both ferromagnetic and antiferromagnetic phases. The plots are total density of states of Mn_3Si (a), Si (b), Mn_I (c), and Mn_{II} (d). The minority spin channel has character similar to a semiconductor.

The band gap in the total dop of AFM ordering is about 0.75 eV which is larger

than than in the FM oder by 0.50 eV. According to Tab. B-1, the magnetic moments in the both Mn_{rmI} and Mn_{rmII} of the parallel spin structure are larger than in the antiparallel alignment. There are large spinpolarizations at the Fermi level for both the FM and the AFM structure.

According to the DOS, the multi-peak Mn_I DOS spreads out in the energy range with considerable intensity. The DOS of Mn_{II} is relatively localized and has two significant peaks: one of them is fully occupied and the other is unoccupied. The exchange splitting of Mn_{II} is larger than for the Mn_I atoms. Consequently, a gap will be opened in the minority spin channel.

★ ★ ★ ★